Temperature independent physisorption kinetics and adsorbate layer compression for Ar adsorbed on Pt(111)

Greg A. Kimmel[1*], Mats Persson[2], Z. Dohnálek[1], and Bruce D. Kay[1]

[1]Pacific Northwest National Laboratory, Environmental Molecular Sciences Laboratory, 902 Battelle Blvd. P.O. Box 999, MSN K8-88, Richland, WA 99352

[2]Dept. of Applied Phys., Chalmers/Göteborg Univ., SE-412 96, Göteborg, Sweden

Abstract

The influence of adlayer compression on the physisorption of Ar on Pt(111) is investigated using temperature programmed desorption and modulated molecular beams. We find that the difference in coverage between the compressed and uncompressed first layers is ~10-15%. For coverages near one monolayer, this compression causes nearly temperature independent desorption kinetics over a wide temperature range (32 K – 41 K). We present a theory that includes the effects of the compression on the desorption kinetics and explains the observed kinetics in terms of a competition between adsorbate-substrate and adsorbate-adsorbate interactions resulting in a continuous increase in the chemical potential near the completion of each successive layer.

[*]Author to whom correspondence should be addressed.

e-mail: gregory.kimmel@pnl.gov

I. Introduction

The adsorption and desorption of weakly bound (physisorbed) atoms and molecules are important fundamental gas-surface processes and therefore have been extensively studied.[1,2] Despite its long history, physisorption still generates significant experimental and theoretical interest.[3,4] Since physisorption does not involve the transfer of electrons between the adsorbate and the substrate, (i.e. no chemical bonds are formed), the lateral corrugation of the adsorbate-substrate interaction (the holding potential) is usually small. As a result, compression effects may play an important role in physisorption. For example, the two-dimensional (2D) structure as a function of coverage is intimately related to the balance between the lateral variation of the adsorbate holding potential and the strength of the distance-dependent interadsorbate interactions. Many previous studies of physisorption at high coverages (i.e. near 1 monolayer) have investigated the structure of adsorbate layers.[1,3,5,6] The variation of the holding potential with distance above the surface also plays an important role in the three-dimensional (3D) adlayer structure for coverages greater than 1 monolayer (ML).

Discussions of desorption kinetics are dominated by an underlying picture that is based on a lattice gas model in which the surface is composed of a fixed number of adsorption sites. In lattice gas models, the corrugation of the holding potential is implied by the structure assumed for the lattice and interadsorbate interactions can be included, but only in a discrete fashion since the distances between adsorbates have specific values as determined by the lattice. Depending on the conditions, a wide range of phenomena can be simulated within lattice gas models (e.g. 2D gases, 2D islands, etc). However, it is difficult to treat the effects of compression within the adsorbate layer with lattice gas models. Surprisingly, relatively few experimental or theoretical investigations on the effect of adlayer compression on desorption have been reported,[7,8] although evidence of compression effects is found in several studies.[9,10]

Bruch and coworkers, have considered the role of compression in adsorption.[11] Using a zero temperature calculation of the minimum energy configuration, they showed that the compression of the first layer raises its chemical potential, and that the bilayer begins forming when the chemical potentials for adsorption of the monolayer and

bilayers are equal. Due to the energy cost for incommensurate adsorption between the adsorbate layers, they assumed that the second layer adsorbed in registry with the first layer. Also, they found that the density of the thin adsorbate layer was equal to the bulk density of the substance and they suggested that these findings should hold in general. The theoretical results agreed well with isothermal adsorption measurements of Xe on Ag(111)[12] which found that the Xe layer compressed as the temperature was decreased under a constant Xe beam flux. The compression of the first layer stopped and the bilayer began forming when the lattice constant of the first layer was equal to the bulk Xe lattice constant.

In this paper, we consider the effects of the compressibility of an adsorbate layer on the adsorption and desorption kinetics of physisorbed atoms from surfaces with high coverages (i.e. ~1 ML or more). In particular, we have investigated the physisorption kinetics of Ar on Pt(111). We find that the compressibility of the Ar adlayers plays an important role in the formation of the adsorbate layer and in the desorption kinetics. We find that the first full Ar monolayer is compressed ~10-15% with respect to the uncompressed first Ar layer. We also find that compression can lead to approximately temperature independent desorption kinetics over a temperature range of ~10 K – a range over which the desorption rate might typically be expected to vary by several orders of magnitude. Based on a quasi-equilibrium argument, we use a thermodynamic approach to calculate the chemical potential of the adsorbate layer as a function of coverage and show that this calculation semi-quantitatively reproduces the observations.

Studying the adsorption of H_2 and D_2 on (1×1)H/Ru(001), Frie*β*, Schlichting, and Menzel[7] observed effects similar to those reported here. In particular, they found that density of adsorbates in the first layer exceeded those of the successive layers and that the binding energy of the first adsorbate layer decreased in the compression region. As we discuss below, the amount of compression of the first adsorbate layer is largely determined by the relative energy difference for adsorption in the first and second layers, and the shape of the adsorbate-adsorbate interaction potential. For H_2 and D_2 on (1×1)H/Ru(001), the authors found that isotope-dependent, zero-point vibration effects played an important role in the adsorbate layer compressibility.[7] For physisorbed gases on Pt, the large van der Waals interaction between the substrate and the adsorbates results

in substantial compression effects in the adlayer. Our results for a heavier ("classical") adsorbate, Ar, at higher temperatures show that the results for H_2 and D_2 adsorption are a limiting case of a more general phenomenon.

II. Experiment

The experiments were performed in an ultra high vacuum (UHV) chamber with a base pressure of ~1×10^{-10} Torr. Two different Pt(111) samples were used, both of which were sputter cleaned and annealed in oxygen and UHV. The sample cleanliness and order were verified with auger electron spectroscopy (AES) and low energy electron diffraction (LEED), respectively. Two different quadrupole mass spectrometers (QMS) could be used to monitor the adsorption and desorption of gases from the Pt(111). The first QMS was a non-differentially pumped, line-of-sight QMS, with an integrating cup[13] whose aperture (1 cm diameter) was approximately 2 cm from the sample. The second was an angle-resolved, rotatable, differentially pumped QMS whose ionizer was approximately 20 cm from the sample. The pump-out time constant for the QMS with the integrating cup is ~20 ms. The sample was cooled with a closed-cycle helium refrigerator, and resistively heated by passing current through a tantalum wire loop to which the sample was spot-welded. The base temperature was ~20 K. The temperature was monitored with a K-type (chromel-alumel) thermocouple spot-welded to the back of the sample. The sample was carefully mounted to minimize temperature gradients. However as discussed below, the analysis of the data suggests the sample had a small, residual temperature gradient of ~0.2 K across it. Gases were deposited on the Pt(111) sample with a supersonic molecular beam. The molecular beam has an in-line shutter that was used to turn the beam on/off with millisecond time resolution.

III. Results and Discussion

Fig. 1 shows several temperature programmed desorption (TPD) spectra for Ar adsorbed on Pt(111). For these spectra, the sample was exposed to successively greater doses of Ar at ~20 K. Distinct peaks in the TPD, characteristic of layer-by-layer

desorption were observed. The peaks at ~48 K, 34 K and 32 K correspond to desorption from the first, second and third layers, respectively. Higher coverages, resulted in multilayer desorption with a common leading edge. This TPD lineshape is characteristic of physisorption for many rare gases adsorbed on metal substrates. The clearly identifiable peaks in this lineshape are caused by the rapidly increasing van der Waals attraction to the Pt substrate for Ar atoms with decreasing distance and that this attraction is stronger than the interaction between the Ar atoms so that Ar wets the Pt substrate. For high coverages (typically greater than 4 ML), the interaction with the substrate is negligible and desorption characteristic of the rare gas solid is observed.

A key feature of the TPD spectra shown in Fig. 1 is the nonzero and approximately constant desorption rate observed between the first and second layer desorption peaks. We will show that desorption in this coverage regime, close to one monolayer, results from decompression of the first monolayer. If the sample temperature is held between approximately 32 K and 42 K during the deposition of the Ar, the formation of the second layer is suppressed, but the compressed monolayer is still formed (data not shown). The origin of the small peak observed in the TPD spectra at ~ 42 K in Fig. 1 is not entirely certain but will be discussed below.

Desorption from the compressed phase has also been studied isothermally. The desorption rate versus time for Ar on Pt(111) for several temperatures is shown in Fig. 2(a). For this data, the Pt(111) was pre-dosed with ~1 ML of Ar at the specified temperature. Then the sample was exposed to a series of 1.5 sec pulses of an atomic Ar beam having a flux of ~0.18 ML/s. The Ar desorption was monitored with the angle-resolved, differentially pumped QMS and signal averaged over 25 Ar pulses. The Ar beam was incident at an angle of 15˚ with respect to the surface normal and the detector was placed at an angle of 30˚ with respect to normal in the backscattering direction. This geometry was chosen to minimize any contribution to the signal from Ar atoms that directly scatter from the surface. Therefore, the signal is representative of atoms that desorb from the surface after trapping. The steady state desorption rate reached near the end of each beam pulse changes slightly as a function of temperature. The differences are primarily due to small changes in the sticking coefficient of the incident Ar atoms as a function of coverage near a monolayer.

The total change in steady state coverage, θ(beam on) - θ(beam off), which is the integral versus time of the difference between the incident flux times the sticking coefficient and the desorption, is ~0.06 ML at 40 K versus ~0.02 ML at 33 K. Surprisingly, when the beam pulse ends, the desorption rate is almost independent of temperature for temperatures between 32-42 K. In fact, the relaxation of the adsorbate layer after the beam pulse ends is somewhat slower at 40 K than at 33 K! Above 42 K, the desorption rate is sufficiently high that the adsorbate layer is no longer compressed by the impinging beam flux. At temperatures below ~32 K, the second layer begins filling since the desorption flux from the fully compressed first layer is lower than the incident beam flux.

The significance of these observations is highlighted by a kinetic analysis of the data. In general, the rate of change of the coverage, is given by,

$$\dot{\theta} = J_{in} S(\theta, T) - J_{des}(\theta, T), \qquad (1)$$

where θ is the coverage, T is the temperature, J_{in} is the flux incident from the gas phase, $J_{des}(\theta,T)$ is the desorption flux and $S(\theta,T)$ is the sticking coefficient. Frequently, the desorption flux is expressed using the Polyani-Wigner equation, $J_{des}(\theta,T) = k_d(\theta,T)\theta^N$, where the N is the desorption order, and k_d is the rate constant. k_d is given by the Arrhenius relation, $k_d(\theta,T) = \nu(\theta)\exp(-E_{des}(\theta)/kT)$, for an activated process, where $\nu(\theta)$ and $E_{des}(\theta)$ are the pre-exponential factor and desorption activation energy, respectively.[14]

If adlayer compression is ignored, then layer-by-layer desorption such as is seen in Fig. 1 suggests that each layer, i, has a distinct desorption energy, E_i, attempt frequency, ν_i, and desorption order, N_i. This "standard" analysis accounts for the general structure of the data in Fig. 1, but fails to reproduce the approximately constant desorption rate observed for Ar adsorbed on Pt(111) between the first and second monolayer desorption peaks. For temperatures just greater than the second layer desorption peak at ~34 K, the observed desorption rate is at least a factor of 100 higher than predicted using the first layer desorption energy.

Fig. 2b shows the isothermal desorption spectra predicted from Eqn. 1 assuming first order desorption kinetics for adsorbates in the second layer (N_2 =1). This calculation

used parameters extracted from fitting the TPD data such as that shown in Fig. 1 (ν_2 = 3.4×10^{13} s^{-1}, E_2 = 0.095 eV). This model predicts that the first layer is completely full and that desorption from it is insignificant on the timescale of the experiments. Prior to the beam pulse, the coverage in the second layer is zero. When the beam pulse begins, the coverage in, and desorption from the second layer begins to increase. At low temperatures (~33 K), the signal is small and the coverage increases quickly since the desorption rate is relatively low. The coverage never reaches a steady state value during the beam pulse and desorption persists long after the end of the beam pulse. At higher temperatures, the signal increases more rapidly and the coverage achieves a steady state value during the beam pulse. Since the steady state coverage is low and the desorption rate is high, the signal quickly drops to zero after the end of the incident beam pulse. Obviously, this model fails to match the experimental observations in even the most qualitative manner.

A similar analysis assuming zero order desorption kinetics for the second layer also fails to reproduce the observations. In that case, the model predicts that the desorption rate is greater than the incident beam flux for all three temperatures. Therefore, the coverage in the second layer would remain essentially zero during the experiment and the isothermal desorption spectra would simply be square waves tracking the incident beam pulse.

For the Ar/Pt(111) system, the desorption features, including the approximately constant desorption rate between the first and second monolayer desorption peaks, can be understood using a statistical approach in which the adsorbate layers are assumed to be in quasi-equilibrium during desorption.[1,14] Typically, quasi-equilibrium can be maintained if the energetic barriers between various configurations of the adsorbate layer are small compared to the desorption energy so that the timescale for desorption is long compared to timescale for the adsorbate layer to equilibrate at a given coverage.[14] In this statistical approach, the desorption rate from an adsorbate layer is obtained by a detailed balance argument. For the case where the adsorbate layer is in equilibrium with a gas (i.e. $\dot{\theta} = 0$), we have from Eqn. (1) that $S(\theta,T)J_{in} = J_{des}(\theta,T)$ and the chemical potentials of the

three-dimensional gas, μ_g^{3D}, and the adsorbates, μ_a, are equal: $\mu_g^{3D} = \mu_a$. Using gas kinetic theory[15] to relate J_{in} to μ_g^{3D}, we can solve for J_{des} in terms of μ_a:

$$J_{des}(\theta,T) = \frac{mS(\theta,T)}{\hbar^3}\left(\frac{kT}{2\pi}\right)^2 \exp\left(\mu_a(\theta,T)\Big/kT\right). \qquad (2)$$

Note that zero and first order kinetics are obtained in this approach when the chemical potential is constant and for a 2D ideal gas, respectively.[1] For the velocities occurring with significant probability in a Maxwellian distribution characteristic of the low temperatures where the Ar desorbs, $S(\theta,T) \sim 1$, independent of the coverage.[16] (For the more energetic atoms in the incident Ar beam, $S(\theta\sim1,T) \approx 0.8$.) Therefore, if quasi-equilibrium is maintained during the desorption, Eqn. 2 allows us to extract the chemical potential of the adsorbate layer from the measured $J_{des}(\theta,T)$ as a function of temperature and coverage.

Fig. 3 shows the chemical potential for Ar on Pt(111) versus Ar coverage extracted from TPD measurements of $J_{des}(\theta,T)$ using Eqn. (2). $\mu_a(\theta,T)$ defines a two-dimensional surface. For a given TPD experiment, the initial coverage and the temperature ramp rate determine the coverage as a function of temperature. Therefore, a TPD experiment traces out a specific trajectory on the surface of $\mu_a(\theta,T)$. We find that varying the TPD ramp rate from 0.5 K/s to 0.05 K/s has only a minor effect on the extracted chemical potential, suggesting that the quasi-equilibrium approximation used in the model is acceptable. The insensitivity of the chemical potential to the TPD ramp rate is supported by the calculations discussed below. Several aspects of the data in Fig. 3, which strongly resemble the results of typical isothermal adsorption measurements,[1] are noteworthy. First, each uncompressed layer desorbs with an approximately constant chemical potential corresponding to zero order desorption. Second, the transition between successive layers is gradual: the regions of constant chemical potential are not connected by vertical steps. The gradual transition between the first and second layer corresponds to the compressed phase (i.e. the region of approximately constant desorption rate between the first and second layers in Fig. 1). Since we have not experimentally determined the absolute coverage, we define 1 ML to be the completion of the compressed monolayer.

With this definition, the coverage of the uncompressed monolayer is ~0.85-0.90 ML.[17] Helium diffraction measurements of Ar adsorbed on Pt(111) have found the lattice constant for a partially compressed monolayer to be ~3.79 Å corresponding to an absolute coverage of 8.04×10^{18} atoms/m^2.[18]

To gain a better understanding of the desorption from the compressed adlayer, we have calculated the chemical potential as a function of coverage and temperature, $\mu_a(\theta,T)$, following the model first introduced by Bruch and Wei.[19] In this scenario, the chemical potential is determined from the chemical potentials of the 2D gas, the various N layer solids, and their coexistence on a flat surface. Here we do not attempt to calculate the chemical potential using the best possible interaction potential model but use a simple model that agrees semi-quantitatively with the experimental results. For the Ar-Ar pair potential, we use the Aziz potential which is derived from gas-phase experiments.[20] Since the Ar overlayer is incommensurate with the Pt(111), adsorption occurs at all points within the Pt(111) surface unit cell.[18] However, our model ignores the corrugation of the Ar-Pt(111) interaction potential. As a result, there is some ambiguity in what value to use for the Ar-Pt interaction potential, $V_{Ar\text{-}Pt}$, in each of the adsorbate layers. Therefore, we have chosen values of $V_{Ar\text{-}Pt}$ for each layer to best fit the TPD data. The value of $V_{Ar\text{-}Pt}(1)$ in the first layer that fits the data, $V_{Ar\text{-}Pt}(1) = -0.100$ eV,[21] is somewhat larger than that used previously to model molecular beam scattering data.[22]

Using these interaction potentials, we have calculated the Helmholtz free energy, $f_s(n_s,T) = \Phi_s(n_s) + f_{vib}(n_s,T)$ per atom for the monolayer, bilayer, and trilayer solids as a function of the atom surface density, n_s, in the first layer. The Helmholtz free energy for the adsorbate layer has contributions from the static lattice sum of the potential energy of the adsorbate layer, $\Phi_s(n_s)$, and a dynamical contribution from the lattice vibrations of the layer, $f_{vib}(n_s, T)$.[19] $\Phi_s(n_s)$ is obtained by summing over the pair-wise interactions of the adsorbates. The free energy associated with the vibrations has been calculated using the quasi-harmonic approximation,[23]

$$f_{vib} = kT\sum_{Q,\nu}\ln(2\sinh(\hbar\omega_{Q,\nu}/2kT) \qquad (3)$$

where the summation runs over all normal modes, Q, and polarizations, ν, in the first Brillouin zone. The chemical potential, $\mu_a(N)$, for the N layer solid and its spreading

pressure, $\phi_a(N)$, which is also needed for the coexistence conditions of the solids, are obtained as

$$\mu_a = \left(\partial \left(n_s f_s(n_s, T) \right) \Big/ \partial n_s \right)_T \text{ and } \phi_a = (N+1) n_s^2 \left(\partial f_s(n_s, T) \Big/ \partial n_s \right)_T . \quad (4)$$

For coverages less than the point where the first layer begins to compress, the model assumes that the adsorbate layer consists of 2D islands in equilibrium with a 2D gas.

In Fig. 3, we make a direct comparison of the calculated chemical potential (dotted line), μ_a, with the chemical potential, μ_a^{TPD}, extracted from the TPD data (solid line). In the calculations, the fully compressed ML corresponds to a surface density of 8.35×10^{18} atoms/m^2. The theory indicates that the change in coverage going from the compressed to uncompressed first layer observed in TPD has contributions primarily from two effects. First, at a fixed temperature, a decrease in coverage is necessary to lower the chemical potential of the compressed first layer to the point where it equals the chemical potential of the uncompressed first layer. Second, as the temperature increases during TPD, the adsorbate layer thermally expands so the coverage corresponding to the uncompressed first layer decreases. Using the Aziz potential, the overall agreement between μ_a and μ_a^{TPD} is relatively good (Fig. 3). However, the calculation underestimates the compressibility of the first adsorbate layer (Fig. 4).

Possible causes of the difference between the observed and calculated compressibility of the first adsorbate layer include the use of the quasi-harmonic approximation, neglect of the many-body van der Waals interactions among the Ar atoms, modifications of the Ar-Ar interaction by the metal substrate, and neglect of the corrugation in the surface potential. The quasi-harmonic approximation overestimates the thermal expansion of the adsorbate layer.[24] Therefore, we might expect a more accurate theory of the thermal expansion to predict less compression than our calculations based on the quasi-harmonic approximation.

Substrate-mediated interactions should weaken the interaction between the Ar adatoms, thus increasing the compressibility of the adsorbate layer. To investigate the influence of the substrate on the Ar-Ar interaction, we have also performed calculations in which the substrate-mediated McLachlan interaction is included.[1] The McLachlan interaction is only appreciable for atoms in the first layer, for adsorbates in higher layers

the interaction potential is nearly identical to the Aziz potential alone. Fig. 4 shows the calculated chemical potential including the McLachlan potential in comparison to the calculation using only the Aziz potential and to the data for coverages near 1 ML. The calculation including the McLachlan interaction is stopped at the point where the layer is no longer compressed since the quasi-harmonic approximation breaks down at that point. (For the calculation without the McLachlan interaction, the theory fails at a higher temperature.) Including the McLachlan interaction does increase the calculated compressibility of the adsorbate layer, improving the agreement between theory and experiment. However, the theory still predicts less compression than is observed experimentally.

The theory including the McLachlan interaction predicts that, during TPD, the temperature at which the adsorbate layer is no longer compressed is ~42 K. This is approximately the temperature where a small peak in the experimental TPD spectra is observed (Fig. 1), suggesting that the peak might be associated with the transition from a compressed to an uncompressed adsorbate layer. We have also observed a similar peak at similar coverages (*relative* to the compressed monolayer) in the TPD spectra of other gases such as Kr and CH_4. In all cases, the peak is sensitive to the Pt crystal quality, preparation and history.[25] A similar feature was previously reported for Xe absorbed on Pt(111) and has been attributed to a compressed to commensurate phase transition.[10] These authors also found that the TPD feature was sensitive to crystal quality. The appearance of this small peak in the TPD spectra for all these different adsorbates suggests a common origin. If the peak is associated with a transition to a commensurate phase, then it must be associated with different commensurate phases for each adsorbate since it occurs at different *absolute* coverages due to the different sizes of the adsorbates. Furthermore, as discussed below, any high-order commensurate phase is likely to be thermally unstable at the temperatures where the peaks appear in the TPD spectra.[6] However to accurately model desorption at these high temperatures, a more advanced treatment of the thermal expansion of the adsorbate layer is required. Such a treatment is beyond the scope of this paper.

For the data in Fig. 3, the apparent coverage of the compressed bilayer is $\theta \approx 1.85$ ML, and the compressed trilayer is $\theta \approx 2.7$ ML. In the model without the McLachlan

interaction, the coverages for the compressed bilayer and trilayer are ~1.95 and ~2.91 ML, respectively. However since we use a molecular beam to deposit the argon, the resulting film has a region of constant coverage in the center (the umbra) and surrounded by a region of decreasing coverage (the penumbra). Detailed simulations of the temperature programmed desorption including both the compression of the adsorbate layer and the penumbra indicate that the penumbra decreases the apparent coverage in the bilayer and trilayer relative to the first layer, in agreement with the observations. Furthermore, at the completion of the both bilayer and the trilayer, the model predicts only a small amount of compression. The apparently larger compression observed experimentally (i.e. the non-vertical steps for the 2^{nd}-3^{rd} and 3^{rd}-4^{th} layer transitions) is most likely due to a small temperature gradient across the sample.[26] In contrast to the transition from the compressed monolayer to the uncompressed monolayer which occurs over ~8 K in the TPD spectra (Fig. 1), the layer transitions at higher coverages occur over a very narrow temperature range (<0.1 K in the model). In those cases, a small temperature gradient across the sample (~0.1-0.2 K) will lead to the apparent broadening of the layer transition versus coverage observed experimentally.

The results in Fig. 3 can readily be understood qualitatively using the theory described above. The sharp decrease in μ_a^{TPD} observed experimentally at very low coverages in Fig. 3 is probably due to adsorption at defects that is not included in the model. Once the defect sites have saturated, the chemical potential is determined by Ar atoms adsorbed on Pt(111) terraces. The attractive van der Waals interactions between these atoms lead to the formation of Ar islands, which coexist with a 2D gas of Ar adatoms. The chemical potential is determined by the equilibrium between the islands and the 2D gas in the holding potential of the substrate. In this coverage range (approximately 0.1 – 0.8 ML), the chemical potential is nearly constant leading to approximately zero order desorption for the uncompressed Ar monolayer. Since the effect of the spreading pressure of the 2D gas on the monolayer solid is negligible, the islands are essentially unconstrained and expand thermally with increasing temperature and decreasing coverage in the TPD experiments. At higher coverages, the fraction of the surface covered with Ar islands is higher. Eventually, the entire surface is covered with

Ar atoms at a density such that the Ar-Ar interaction energy is minimized corresponding to an uncompressed monolayer at ~0.87 ML.

For coverages greater than ~0.87 ML, we might expect adsorption in the second layer. However, the adsorbate-substrate interaction is considerably weaker for the second layer and therefore it is energetically favorable to increase the coverage in the first layer. The Ar-Ar distance between adsorbates in the layer decreases below the optimum and the atoms begin to sample the repulsive wall of their neighbors, thereby increasing the chemical potential of *all* the adsorbates. The second adsorbate layer forms when the chemical potential of the compressed first layer equals that of the uncompressed bilayer, that is, when it is no longer energetically favorable to further compress the first layer.[11,19] The calculation using only the Aziz potential for the Ar-Ar interaction predicts the change of coverage going from the fully compressed monolayer to the uncompressed monolayer of about 0.07 ML and is about half of the compression seen experimentally (Fig. 4). With the McLachlan interaction included, the calculated change in coverage as the first layer compresses is ~0.11 ML (Fig. 4).

For 1.0 ML < θ < 1.95 ML, the Ar film consists of a compressed monolayer solid coexisting with a bilayer solid. At θ ~ 1.95 ML where the bilayer is complete, additional adsorption results in compression of the bilayer and an increase in the chemical potential for all the adsorbates. However, since the chemical potential difference between the second and third layers is relatively small, the calculated compression of the bilayer is small (~0.01-0.02 ML). For 1.95 ML < θ < 2.91 ML, the film corresponds to the coexistence of a bilayer and a trilayer solid. Due to the small temperature range in TPD during which the second and third layers desorb, μ_a is essentially constant in these coexistence regions. The surface densities of the bilayer solid in coexistence with the monolayer and trilayer solids determine the boundaries of the transition region between the uncompressed and the compressed bilayer solid.

Fig. 5 compares the TPD spectra calculated both with and without the McLachlan interaction to a typical TPD spectrum taken from Fig. 1. (The TPD for the model including the McLachlan interaction is not calculated for T > 42 K where the model breaks down.) The models are able to reproduce the nearly constant rate observed between the desorption peaks for the first and second layers, and give nearly quantitative

agreement with the experimentally observed desorption rates. However since the models underestimate the compressibility of the adsorbate layer, they also underestimate the desorption rate from the compressed first layer.

The quasi-equilibrium model can also be used to explain several of the characteristic features in the isothermal desorption experiments (Fig. 2a). In those experiments, the initial coverage (i.e. just prior to each beam pulse) corresponds to a partially compressed monolayer. When the Ar beam pulse turns on, the desorption rate is initially low compared to the incident flux and therefore the coverage increases. The additional adsorbates increase the compression of the first layer, raising the chemical potential, and causing an increase in the desorption rate. At higher temperatures, the initial coverage is lower and therefore more compression is required to raise the chemical potential to the value defined by the incident Ar beam flux. Therefore, it takes longer for the desorption rate to increase. For the beam fluxes used in the experiments and temperatures between approximately 32 and 42 K, the coverage increases until the desorption rate equals the adsorption rate. The steady state coverage achieved during the pulse depends on the temperature but is close to 1 ML. When the beam pulse ends, the change in the desorption rate – which is approximately independent of temperature – is also governed by the change in the chemical potential as the coverage decreases.

Fig. 6 compares the experimental isothermal desorption spectra to those calculated using the Aziz and McLachlan potentials. The model semi-quantitatively reproduces the experimental observations. Since the model underestimates the compressibility of the adsorbate layer, the desorption rates in the simulated spectra increase more quickly after the beam pulse starts than is observed experimentally. However, the model correctly predicts the slower relaxation observed at higher temperatures after the beam pulse ends. This is in stark contrast to the waveforms calculated for incompressible adsorption as shown previously in Fig. 2b.

Due to the stronger Ar-Pt interaction for Ar atoms in the first layer, we might expect the density of the compressed first layer to exceed the density of the higher layers. Experimentally however, the density in the compressed monolayer is generally equal to the density of the bilayer.[12,19] This observation has been explained by noting that the energy cost for having incommensurate adlayers is too high.[11] Another factor however,

is that the substrate weakens the interaction between adsorbates in the first layer (the McLachlan interaction), increasing the lattice constant of the uncompressed first monolayer relative to the lattice constant of the second adsorbate layer where the substrate-mediated interactions are small. As a result, even in the absence of registry effects between the adlayers, the density of the compressed first layer would be comparable to the density of the uncompressed second layer.

Previous experiments using helium scattering have identified high-order commensurate phases for Kr[5] and Ar[6] adsorbed on Pt(111) which are "locked" with respect to the substrate. At low temperatures, the helium diffraction spectra show clear evidence of coexisting domains with different lattice constants. For these experiments, the thermal expansion of the adsorbate layer was also measured for various sub-monolayer coverages. For Ar on Pt(111) for 0.85 ML < θ < 1.0 ML, the Ar lattice constant of the higher density commensurate phase was found to be independent of temperature for T < 35 K.[6] The method used for measuring the adsorbate coverage in these papers, is consistent with, and should give the same relative coverage as, the method used here. The range of coverages over which the higher density phase was observed at low temperatures agrees well with the range of coverages for which we observed the compressed monolayer in desorption. The observation that the overlayer lattice constant does not change with temperature was presented as strong evidence for the high-order commensurate phase since these overlayers were "locked" to the Pt(111) substrate.

The helium diffraction data might appear to contradict the data presented here. However as the authors note, high-order commensurate phases are probably destabilized by thermal fluctuations at temperatures were desorption is appreciable.[6] Futhermore, while we agree with the earlier identification of the high-order commensurate phases for Kr and Ar, we note that in both cases the measurements of the lattice constant of the "locked" adlayer as a function of temperature were made at coverages where the monolayer is compressed. Therefore, if the temperature is low enough that desorption is negligible, even an incommensurate layer will not expand with temperature since there is no room for expansion. In fact for Ar, the lattice constant was found to increase for

temperature above ~35 K[6] which is in the temperature range where desorption from the compressed phase is observed in our experiments.

It is well known that at intermediate coverages island formation can result in zero order desorption kinetics for adsorbates in the first layer.[27] At low coverages, the adsorbates form a 2D gas and first order desorption kinetics are typically found. However, zero order desorption kinetics are also typically observed for desorption occurring from the second layer, even when the coverage in the second layer is small and first order kinetics might naively be expected. Zero order desorption kinetics naturally emerge once the compression of the adsorbate layer is included. In that case, the chemical potential of the adsorbates in the monolayer and bilayer are equal and the number of adsorbates available for desorption is constant so long as the bilayer coverage is greater than zero.

The theory used to describe the desorption from the compressed phase is based on the assumption that the system maintains quasi-equilibrium. The semi-quantitative agreement between the theory and the data suggests that this is a good assumption. However, the quasi-equilibrium assumption can break down. For example, depending on how adsorbate layers with total coverages near one monolayer are prepared, we can observe desorption from the second monolayer prior to the completion of the fully compressed first monolayer, but never without some compression of the first layer.

IV. Conclusions

In summary, we have carried out a combined experimental and theoretical study of the physisorption kinetics of Ar on Pt(111). The measured temperature programmed and isothermal desorption spectra were analyzed with a statistical approach in terms of the chemical potential that was calculated using simple interaction potential models. This statistical approach is based on the assumption that the system is in quasi-equilibrium, which is justified by the low energy barriers between various configurations of the physisorbed adsorbates. We find that the compression of the adsorbate layer and the corresponding increase in the chemical potential of the adsorbates plays an important role in the physisorption kinetics. For example, we have also observed the formation of the

compressed monolayer for a number of other gases (N_2, O_2, CH_4, Kr, etc) on Pt(111) and other surfaces such as MgO(001). These results will be presented in a future publication.

Acknowledgements

GAK, BDK and ZD were supported by the U.S. Department of Energy Office of Basic Energy Sciences, Chemical Sciences Division. Part of the research was performed at the W.R. Wiley Environmental Molecular Science Laboratory, a national scientific user facility sponsored by the Department of Energy's Office of Biological and Environmental Research and located at the Pacific Northwest National Laboratory. Pacific Northwest National Laboratory is operated for the U.S. Department of Energy by Battelle under Contract DE-AC06-76RLO 1830. MP is grateful for support from the Swedish Research Council (VR) and for the hospitality of the Institute of Surface, and Interface Science (ISIS) at UC Irvine, where part of this research was carried out.

Figure Captions:

Fig. 1. Desorption rate versus temperature for Ar adsorbed on Pt(111). The spectra were obtained with a line-of-sight QMS using a TPD ramp rate of 0.25 K/s. The peaks at ~48 K, 34 K and 32 K correspond to desorption from the first, second and third layers, respectively. The nearly temperature independent desorption from 34 K – 41 K corresponds to desorption from the compressed first layer.

Fig. 2. Isothermal Ar desorption rate versus time. a) For the experiments, a monolayer of Ar was prepared on the Pt(111) crystal. The temperature was held constant, the sample was exposed to a 1.50 s pulse of Ar atoms, and the desorbing Ar was monitored. The Ar beam was incident at angle of $\theta_{in} = 15^{o}$ and the desorbing atoms were detected at $\theta_{des} = 30^{o}$. The delays in desorption at the beginning of the beam pulses and the nearly temperature independent desorption after the beam pulses are due to the compression of the adsorbate layer. b) A simple model assuming first order desorption kinetics (see text) fails to reproduce the observations. The model curves have been offset for clarity.

Fig. 3. Chemical potential, $\mu_a(\theta,T)$, for Ar on Pt(111) versus coverage. The chemical potential extracted from an experimental TPD spectrum with a ramp rate of 0.25 K/s is shown. The calculated chemical potential using the Aziz potential semi-quantitatively reproduces the experimental observations.

Fig. 4. Chemical potential, $\mu_a(\theta,T)$, for Ar on Pt(111) versus coverage near 1 ML. The chemical potential calculated from two different TPD spectra are shown. These spectra differ in the size of the small peak seen at ~42 K in the TPD (see Fig. 1). The two data sets are included to indicate the typical range of results obtained when converting the TPD spectra to $\mu_a(\theta,T)$. Calculated chemical potentials using the Aziz potential and the Aziz plus the McLachlan potential are also shown. The calculation including the McLachlan potential predicts more compression than the calculation that only includes the Aziz potential.

Fig. 5. Experimental and calculated TPD spectra. The calculated TPD spectra semi-quantitatively reproduce the experimental observations, including the nearly temperature independent desorption from the compressed first monolayer from 34 K – 41 K. Since the calculation including the McLachlan potential predicts more compression than the calculation with only the Aziz potential, it predicts a higher desorption rate from the compressed monolayer. The calculation including the McLachlan potential is stopped when the monolayer finishes decompressing and the calculation breaks down.

Fig. 6. Isothermal Ar desorption rate versus time. a) Experimental results (same as Fig. 2a). b) The isothermal desorption spectra calculated assuming quasi-equilibrium, and using the Aziz and McLachlan potentials agree semi-quantitatively with the data, reproducing the nearly temperature independent desorption observed experimentally. The calculated isothermal spectra have been offset for clarity.

References:

[1] L. W. Bruch, M. W. Cole, and E. Zaremba, *Physical Adsorption: Forces and Phenomena*. (Clarendon Press, Oxford, 1997).

[2] H. J. Kreuzer and Z. W. Gortel, *Physisorption Kinetics*. (Springer-Verlag, Berlin, 1986).

[3] B. Grimm, H. Hovel, M. Pollmann, and B. Reihl, Phys. Rev. Lett. **83** (5), 991 (1999).

[4] W. J. Weber and D. L. Goodstein, Phys. Rev. Lett. **83** (19), 3888 (1999); F. Celestini, D. Passerone, F. Ercolessi, and E. Tosatti, Phys. Rev. Lett. **84** (10), 2203 (2000).

[5] K. Kern, P. Zeppenfeld, R. David, and G. Comsa, Phys. Rev. Lett. **59** (1), 79 (1987).

[6] P. Zeppenfeld, U. Becher, K. Kern, and G. Comsa, Phys. Rev. B **45** (10), 5179 (1992).

[7] W. Frieβ, H. Schlichting, and D. Menzel, Phys. Rev. Lett. **74** (7), 1147 (1995).

[8] V. P. Zhdanov, J. Chem. Phys. **95** (3), 2162 (1991).

[9] H. Schlichting and D. Menzel, Rev. Sci. Inst. **64** (7), 2013 (1993).

[10] W. Widdra, P. Trischberger, W. Frieβ, D. Menzel, S. H. Payne, and H. J. Kreuzer, Phys. Rev. B **57** (7), 4111 (1998).

[11] L. W. Bruch, J. Unguris, and M. B. Webb, Surf. Sci. **87**, 437 (1979).

[12] J. Unguris, L. W. Bruch, E. R. Moog, and M. B. Webb, Surf. Sci. **87**, 415 (1979).

[13] H. Schlichting and D. Menzel, Surf. Sci. **285**, 209 (1993).

[14] H. J. Kreuzer and S. H. Payne, in *Dynamics of Gas-Surface Interactions*, edited by C. T. Rettner and M. N. R. Ashfold (The Royal Society of Chemistry, London, 1991), pp. 366.

[15] F. Reif, *Fundamentals of statistical and thermal physics*. (McGraw-Hill, Boston, 1965).

[16] M. Head-Gordon, J. C. Tully, C. T. Rettner, C. B. Mullins, and D. J. Auerbach, J. Chem. Phys. **94** (2), 1516 (1991); M. Head-Gordon, J. C. Tully, H. Schlichting, and D. Menzel, J. Chem. Phys. **95**, 9266 (1991).

[17] We find that the coverage of the uncompressed monolayer depends somewhat on both the particular Pt(111) crystal, the sample cleaning procedure used, and the number of TPD spectra obtained since the last sample cleaning. In all cases, the samples have a good LEED patterns with no contamination detectable with AES. We attribute these minor differences to effects such as different distributions of terrace widths and steps between samples and very low levels of contaminants.

[18] L. W. Bruch, A. P. Graham, and J. P. Toennies, J. Chem. Phys. **112** (7), 3314 (2000).

[19] L. W. Bruch and M. S. Wei, Surf. Sci. **100**, 481 (1980).

[20] R. A. Aziz and M. J. Slaman, Molec. Phys. **58**, 679 (1986).

[21] The values used the Ar-Pt interaction for layers i=2,3 and 4 are -0.0593, -0.0537 and -0.0525 eV, respectively.

[22] D. Kulginov, M. Persson, C. T. Rettner, and D. S. Bethune, J. Phys. Chem. **100**, 7919 (1996).

[23] G. P. Srivastava, *The Physics of Phonons*. (Adam Hilger, Bristol, 1990).

[24] J. M. Phillips, L. W. Bruch, and R. D. Murphy, J. Chem. Phys. **75** (10), 5097 (1981).

[25] In Fig 1, the magnitude of the small peak at ~42 K is seen to vary considerably even though no contamination is detectable in Auger electron spectroscopy in any of the spectra.

[26] Another possible source of broadening in the layer transitions is due to the pumping time constant for the mass spectrometer. However, by using a slower temperature ramp, this potential source of error was ruled out.

[27] P. J. Estrup, E. F. Greene, M. J. Cardillo, and J. C. Tully, J. Phys. Chem. **90** (17), 4099 (1986).

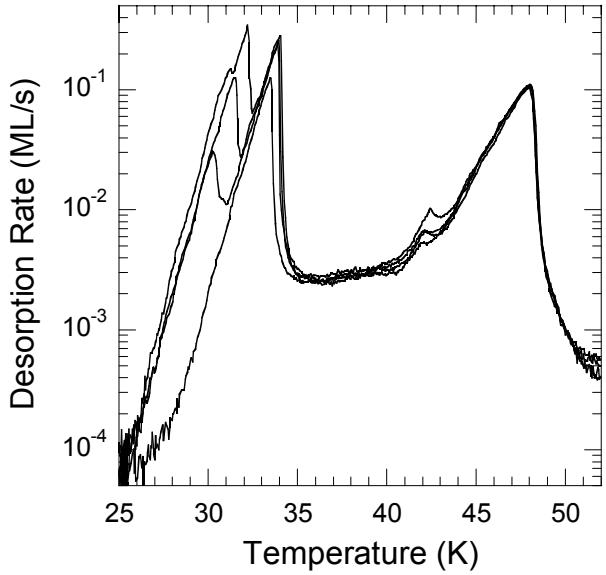

Fig. 1
Kimmel, et al.
J. Chem. Phys.

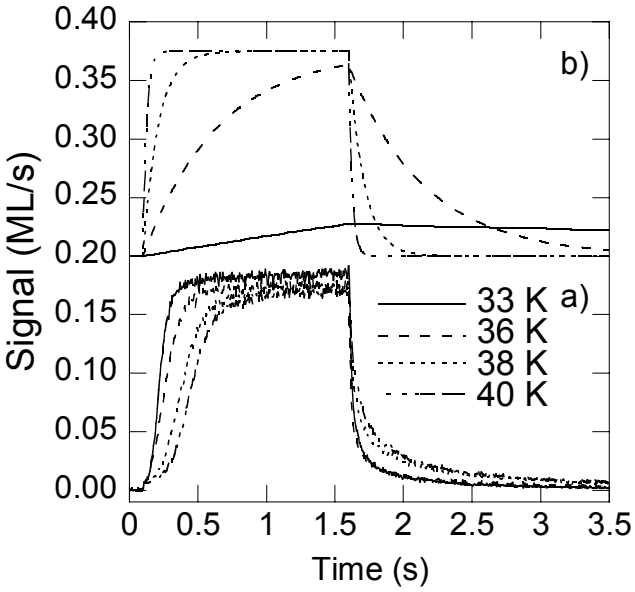

Fig. 2
Kimmel, et al.
J. Chem. Phys.

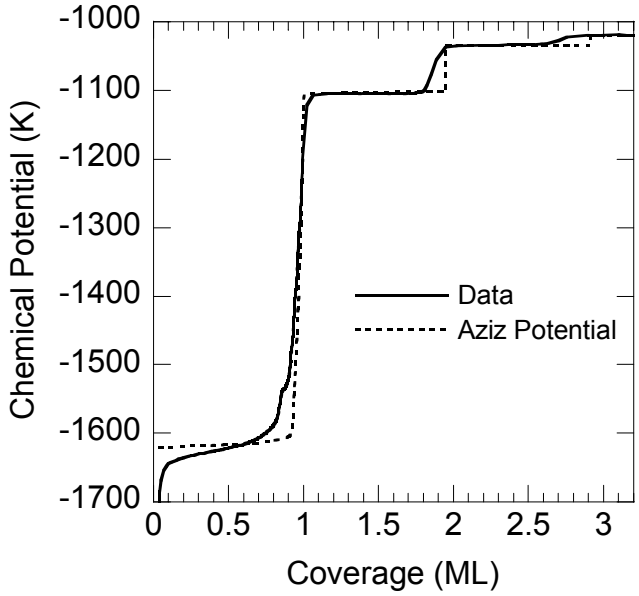

Fig. 3
Kimmel, et al.
J. Chem. Phys.

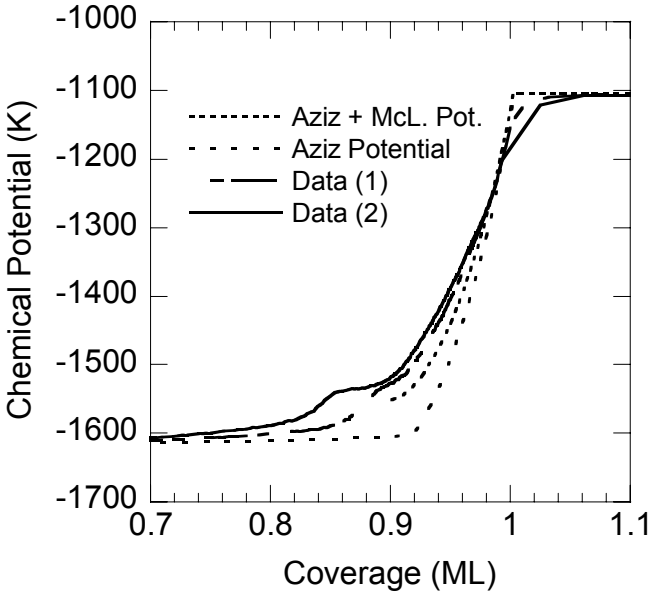

Fig. 4
Kimmel, et al.
J. Chem. Phys.

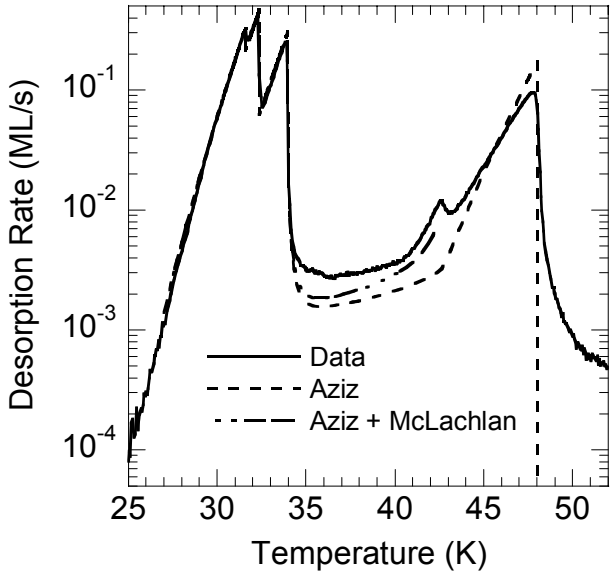

Fig. 5
Kimmel, et al.
J. Chem. Phys.

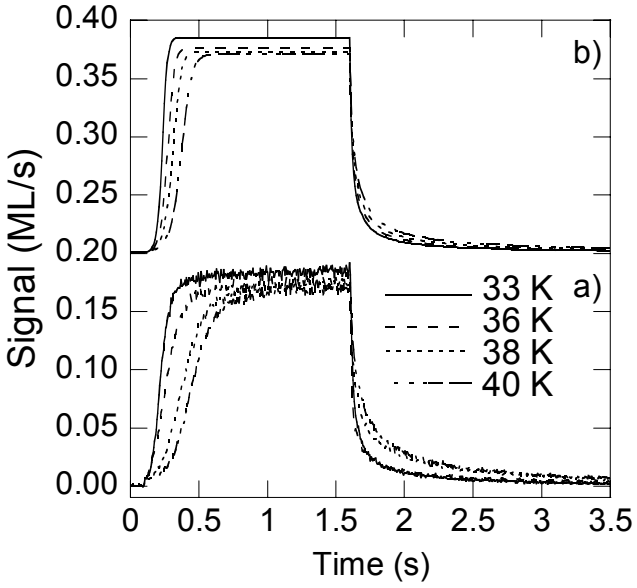

Fig. 6
Kimmel, et al.
J. Chem. Phys.